Cosmology, Galaxy Formation and Astroparticle Physics
on the pathway to the SKA
Klöckner, H.-R., Rawlings, S., Jarvis, M. & Taylor, A. (eds.)
April 10th-12th 2006, Oxford, United Kingdom

The Dark Energy Survey

J. Weller[1], J. Frieman[2,3], O. Lahav[1] and Z. Ma[4]
for the DES collaboration

[1] Department of Physics & Astronomy, University College London, Gower Street, London WC1E 6BT, U.K.
[2] Particle Astrophysics Center, Fermilab National Accelerator Laboratory, Batavia, IL-60510-0500, USA
[3] Kavli Institute for Cosmological Physics and Department of Astronomy & Astrophysics, The University of Chicago, Chicago, IL 60637
[4] Department of Physics and Astronomy, University of Pennsylvania, Philadelphia PA 19104

Abstract. The Dark Energy Survey is proposing to constrain dark energy with four complementary probes: galaxy cluster counts, weak lensing, galaxy clustering and Type Ia Supernovae. In order to achieve this a new 3 deg^2 CCD camera will be mounted on the Blanco 4-m telescope at the Cerro Tololo Inter-American Observatory (CTIO). The camera will be sensitive up to 24$^{\rm th}$ magnitude in the g,r,i and z bands. The proposed observation will cover 5,000 deg^2 of the sky and overlap with the field of the South Pole Telescope (SPT), which will perform a blind survey of galaxy clusters, selected by their Sunyaev-Zel'dovich decrement. The specifications of DES will allow to constrain the equation of state parameter of dark energy to better then a few percent. accuracy.

1. Introduction

One of the biggest challenges in modern cosmology is to reveal the cause of accelerated expansion of the Universe. There are three possible explanations for the observed accelerated expansion: Firstly there is an additional component in the energy-momentum tensor, namely *dark energy*, which has a pressure $p_{\rm DE} \leq -\rho_{\rm DE}/3$, secondly gravity could be modified on large scales and thirdly an inhomogeneous Universe. The 'simplest' model to fit the data is a Universe with a Cosmological Constant, although this then comes with the problem of the need to explain the origin of the observed value with fundamental physics.

The first question surveys need to answer is if the dark energy is observationally distinguishable from a Cosmological Constant? In order to decide this one has to measure the equation of state $w = p_{\rm DE}/\rho_{\rm DE}$ possibly at different redshifts. A Cosmological Constant corresponds to $w = -1$. A further question is, is it possible to distinguish modifications of gravity from a dark energy component and finally in the case of $w \neq -1$ is evolving with redshift? In the following we choose $w = w_0 + w_a(1-a)$ as the parameterization for the equation of state (Linder 2003).

There are many means to probe cosmology in the Universe, but the majority of them fall in two categories. First there are geometrical probes, which mainly probe the different weights of the comoving distance

$$r(z) = \int \frac{dz}{H(z)} \qquad (1)$$

where $H(z)$ is the Hubble parameter given in standard gravity at late times by $H^2(z) = H_0^2\left[\Omega_{\rm m}(1+z)^3 + \Omega_{\rm DE}(1+z)^{3(1+w)}\right]$, in a flat Universe with a constant equation of state factor w. Geometrical probes are then standard candles, i.e. probes of the luminosity distance $d_L = (1+z)r(z)$, standard rulers which probes the angular diameter distance $d_A = (1+z)^{-1}r(z)$ or probes of the volume $dV/(dz\, d\Omega) = r^2(z)H(z)$. Secondly there are probes of the growth factor

$$D'' + D'\left[\frac{3}{a} + \frac{H'}{H}\right] = \frac{3}{2}\frac{H_0^2}{H^2}a^{-5}\Omega_m D\ , \qquad (2)$$

with D the fluctuation in the matter component and primes denoting derivatives with respect to the scale factor a. Usually in modified gravity scenarios the term on the right is modified.

The majority of the material presented in the following sections is discussed in detail in the report (The Dark Energy Survey Collaboration 2005) submitted to the Dark Energy Task Force (DEFT; Albrecht et al. 2006). The international DES collaboration includes universities from the US, UK, Spain, and Brazil. The DES:UK consortium (UCL, Portsmouth, Cambridge, Edinburgh and Sussex) has now received support from PPARC towards the wide field optical corrector for DES.

2. The Instrument and Survey

The main challenge for the DES collaboration is to build a new camera and corrector for the 4m Blanco telescope. The major components are a 519 megapixel CCD camera a wide field optical corrector with 2.2 degree field of view, a four band filter system with g,r,i and z filters, guide and focus sensors mounted on the focal plane, low-noise CCD readout, a cryogenic cooling system to maintain the focal plane at 180 K, as well as a data acquisition and instrument control system to connect to the Blanco observatory infrastructure. The camera focal plane will consist of sixty-two 2k x 4k CCDs (0.27"/pixel) arranged in a hexagon covering an imaging area of 3 square degrees. Smaller for-

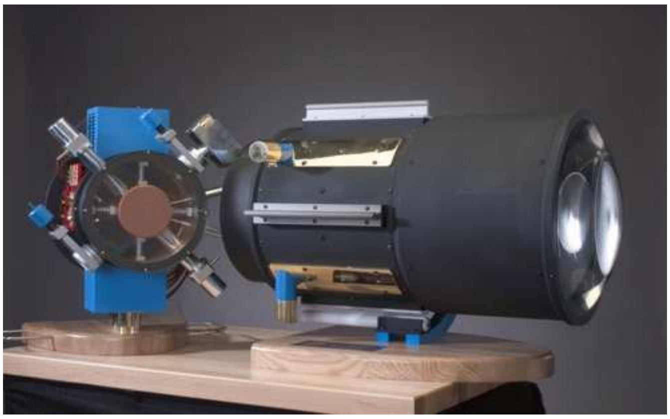

Fig. 1. Model of the Dark Energy Camera (DECam).

mat CCDs for guiding and focusing will be located at the edges of the focal plane.

To carry out the Dark Energy Survey, we have requested 525 nights of observing on the Blanco telescope over 5 years, concentrated between September and February, beginning in Sept. 2009. With that time, we expect to reach photometric limits of g=24.6, r=24.1, i=24.3, and z=23.9 over 5000 square degrees of sky. These are 10σ limits in 1.5" apertures assuming 0.9" seeing and are appropriate for faint galaxies; the corresponding 5σ limit for point sources is 1.5 mags fainter. These limits and the adopted median delivered seeing are derived from detailed survey simulations that incorporate weather and seeing data at CTIO over a 30-year baseline.

The survey strategy is designed to optimize the photometric calibration by tiling each region of the survey with at least four overlapping pointings in each band. This provides uniformity of coverage and control of systematic photometric errors via relative photometry on scales up to the survey size. This strategy will enable us to determine photometric redshifts (photo-z's) of galaxies to an accuracy of $\sigma(z) \sim 0.07$, with some dependence on redshift and galaxy type, cluster photometric redshifts to $\sigma(z) \sim 0.02$ or better out to $z \sim 1.3$, and shapes for approximately 200 million galaxies; these measurements will be sufficient to meet the survey science requirements. 4000 $\deg^2$ of the survey region will overlap with the South Pole Telescope (Ruhl et al. 2004) Sunyaev-Zel'dovich survey region; the remainder will provide coverage of spectroscopic redshift training sets, including the SDSS southern equatorial stripe, and more complete coverage near the South Galactic pole. In order to extract cosmology from the dark energy survey a certain accuracy in the photometric redshifts is required. This is achieved by measuring the relative flux in the g,r,i and z filters to determine the 4000Å break.

3. The Cosmological Probes

3.1. Galaxy Cluster Counts

The SPT will observe 4,000 $\deg^2$ of sky in the southern hemisphere with a 10-m telescope equipped with a 1,000 bolometer array in its focal plane (Ruhl et al. 2004). It consists of a 1 arcminute beam and operates in 3-4 frequency bands at (90), 150, 250 and 270 GHz. This will allow blind observations of galaxy clusters selected by the Sunyaev-Zel'dovich decrement. Given the complementary redshift information from DES it is then possible to count clusters of galaxies in bins of redshift. This can be compared to theoretical predictions of structure formation with

$$\Delta N = \Delta\Omega \int_{z_{\rm bin}} dz \frac{dV}{dz d\Omega} \int_{M_{\rm lim}(z)}^{\infty} \frac{dn}{dM}\, dM \ , \qquad (3)$$

where $\Delta\Omega$ is the survey area, dn/dM the mass function and $M_{\rm lim}(z)$ the selection function depending on the survey parameters, cosmological parameters and the gas physics in the cluster. The sensitivity of the SPT is about 1.5 mJy for a 4-σ detection threshold of a cluster. This corresponds to a limiting mass of $1.7 \times 10^{14} M_\odot$, also this number varies slightly with redshift. Typically the mass function is established with N-body simulations (Jenkins et al. 2001) and fit to analytical expression such as the Sheth-Tormen mass function (Sheth & Tormen 2002). The most commonly used mass function by (Jenkins et al. 2001) is given by

$$\begin{aligned} \frac{dn}{dM}(z, M) \ = \ & -0.316 \frac{\rho_m(t_0)}{M} \frac{d\sigma_M}{dM} \frac{1}{\sigma_M} \\ & \times \exp\left\{-|0.67 - \log\left[D(z)\sigma_M\right]|^{3.82}\right\} \ , \end{aligned} \qquad (4)$$

with σ_M the rms fluctuation on mass scale M, $D(z)$ the growth factor of linear perturbations and $\rho_m(t_0)$ the matter density today. In order to predict the number of cluster in redshift bins we convert the Sunyaev-Zel'dovich flux limit of the survey to a mass limit. For this we assume a relation between mass and temperature, which allows deviations from hydrostatic equilibrium (Verde et al. 2002; Battye & Weller 2003) with a temperature relation of

$$T_e = T_* \Delta_c^{1/3} H(z)^{2/3} (1+z)^{1-\epsilon} M_{\rm vir}^{1/\xi} \ , \qquad (5)$$

where T_* is the normalization, Δ_c the spherical overdensity of the cluster at virialization, ϵ the redshift dependence and ξ the power-law for the variation with mass. Assuming virialization would result in $\epsilon = 1$ and $\xi = 1.5$. We use $T_* = 1.6$ as motivated by hydro simulations (Battye & Weller 2003). Also a deviation from virialization might be expected if it turns out that clusters with masses larger than $10^{14} M_\odot$ follow relatively closely the scaling relation from virialization (Motl et al. 2005; Nagai 2006). We include the parameters T_*, ξ and ϵ as free parameters in the cluster count analysis, which leads to a self-calibration of these parameters (Hu 2003; Majumdar & Mohr 2004; Lima & Hu 2004). Furthermore we also calibrate these parameters with DES cluster weak lensing observations (Huterer & White 2002; Sealfon et al. 2006; Dodelson et al. 2007). For this we assume 15 galaxies per square arcminute with a distribution of $dn/dz = ze^{-z/z_c}$, with $z_c = 0.5$. We choose a bin-width of $\Delta z = 0.1$ and stack clusters within SZ flux decrement bins of $3\Delta S_\nu = 1140\mu$Jy. If we assume a value of $\sigma_8 = 0.9$ we can then calibrate T_*, ξ and ϵ with accuracies of $\Delta T_* = 1.1$, $\Delta\xi = 0.05$ and $\Delta\epsilon = 0.07$.

Since the total number of clusters observed to $z_{\max} = 1.5$ goes down from $\approx 21,000$ cluster for $\sigma_8 = 0.9$ to $\approx 5,600$ clusters for $\sigma_8 = 0.75$ we degrade the errorbars in the covariance matrix of T_*, ξ and ϵ by a factor of $\sqrt{3.7}$ for the lower value of σ_8. While the weak lensing calibration does not improve constraints on T_* significantly compared to calibration with the cluster counts themselves, the redshift and mass power-law parameters ξ and ϵ are more tighter constrained by the weak lensing calibration. We should note that the clustering of clusters provides another useful calibration of the mass-temperature relation (Majumdar & Mohr 2004), but we have not implemented this in the analysis presented here. In order to predict the redshift distribution of the SZ clusters we also allow beam degradation up to 20 arcmin (above which the primary CMB adds too much noise), but do neglect point source confusion noise.

3.2. Weak Lensing

The observed shapes of galaxies is distorted by the large scale matter distribution along the line of sight. Large scale structure hence generates a correlated shear pattern, which can be analysed statistically in the shear-shear correlation. Since foreground galaxy positions are also correlated to the large scale structure, one can also study galaxy-shear correlations. This leads to a projected power spectrum, which in the case of the shear-shear correlation is given by

$$C_l^{\gamma\gamma} = \int dz \frac{H(z)}{d_{\rm A}(z)^2} W_\gamma^2(z) P(k = l/d_{\rm A}; z) \ , \qquad (6)$$

with $W_\gamma(z)$ a weighting function and $P(k)$ the three dimensional matter power spectrum. The dark energy density and equation of state affect these angular power spectra through the Hubble parameter, the angular diameter distance, the weight factors, and through the redshift- and scale dependence of the three-dimensional power spectra $P(k)$. Note that we can extract additional information by obtaining the spectra at different redshift bins, which provides weak lensing tomography. We can predict the error in the angular power spectrum (Kaiser 1992) with

$$\Delta C_l^{\gamma\gamma} = \sqrt{\frac{2}{(2l+1) f_{\rm sky}}} \left(C_l^{\gamma\gamma} + \frac{\sigma^2(\gamma_i)}{n_{gal}} \right) \ , \qquad (7)$$

where $f_{\rm sky}$ is the fraction of sky covered, $\sigma(\gamma_i)$ is the single component variance and n_{gal} is the density of source galaxies per steradian. For the analysis presented here, we assume $A_{\rm sky} = 5,000\,{\rm deg}^2$, a median redshift of the galaxy distribution at $z_{\rm med} = 0.68$ and $n_{\rm gal} = 12$ arcmin^{-2}, which is obtained by assuming a median delivered seeing of $0.9''$. However we also have to include possible systematic errors in the analysis. One important effect to include is bias and scatter in the measured photometric redshift (Ma et al. 2006; Huterer et al. 2006). We introduce 41 bias and 41 scatter parameters to include systematic errors for the photometric redshifts. We assume that these parameters can be 'trained' to 0.002 prior accuracy. It was shown by Ma et al. (2006) that a training set of 50,000-100,000 galaxies reaching DES depth can achieve this accuracy. For forecasting the weak lensing survey of DES we assume 7 distinct tomography bins between redshift $z = 0$ and $z = 2$ and an $l_{\max} = 1000$. In addition to the redshift error there are also shape measurement errors, which can be caused by anisotropies in the point spread function (PSF). This problem can be minimised by measuring the PSF to high accuracy. Recently the error in measuring the PSF shape has been substantially reduced by introducing a Principal Component Analysis (PCA) technique that optimally uses information on the PSF from multiple exposures (Jarvis & Jain 2004); this enables interpolation of the PSF with much finer effective angular resolution. The estimated residuals for DES are well below the statistical errors. Hence we believe that additive errors in the estimated shear will be negligible in the error budget of DES lensing measurements.

3.3. Galaxy Clustering

DES will obtain the images and redshifts of about 300 million galaxies. Hence DES can obtain a precise measurement of galaxy power spectrum, which is related to the underlying mass distribution via a scale and redshift dependent bias parameter. However, on large scales we expect the bias $b^2(z)$ to be only redshift dependent

$$P_{\rm gal}(k, z) \propto k^n T^2(k) D^2(z) b^2(z) \ , \qquad (8)$$

with, as before, n the primordial spectral index, $T(k)$ the transfer function and $D(z)$ the growth factor. In practice this simple bias model is replaced by a halo occupation model (The Dark Energy Survey Collaboration 2005). The galaxy power spectrum includes characteristic scales, namely the turn over is related to matter-radiation equality, and the pressure of baryons imprints wiggles on characteristic scales, related to the baryon acoustic oscillations (BAO). These scales can be exploited as standard rulers (Cooray et al. 2001). Due to the errors in redshift it is not feasible to measure a full three-dimensional power spectrum. We will hence analyse the angular correlation function within redshift shells

$$C_{\rm gal}^i(l) = \frac{2}{\pi} \int_0^\infty k^2 \, dk \, f_i^2(k, l) P_{\rm gal}(k, 0) \ , \qquad (9)$$

with f_i the Bessel transform of the radial selection function for redshift shell i integrated over the growth. We use the same survey specifications as in the weak lensing section. In addition we use one galaxy bias parameter in each redshift bin. We assume that the galaxy power spectrum and BAO oscillation are measured up to angular multipoles of $l_{\max} = 300$.

3.4. *Type Ia Supernovae*

10% of the time dedicated to DES, will be used for Supernovae observations in 40 $\deg^2$. The requirements of this design include the production of a large number of well-sampled SNe light curves in three bands and an observing strategy which fits within the 5,000 $\deg^2$ DES survey area and survey strategy. Based on previous modeling, balancing desired spatial coverage with desired depth to cover a wide range of redshifts ($0.25 < z < 0.75$), we have selected exposure times of 200s in r, 400s in i, and 400s in z. The r images will detect SNe and measure their light curves. The i and z band images will provide color information for SN typing and determination of SN photometric redshifts. Stacked images will provide very deep photometry of the host galaxies. We used 2,200 SNe and assumed for the moment spectroscopic redshifts for the forecasts. A more realistic approach is currently being developed. We assume two Gaussian distributed subsamples of SNe, with one consisting of 200 at $z_{\rm med} = 0.2$ and $\sigma_z = 0.15$ and the other with 2,000 at $z_{\rm med} = 0.5$ with $\sigma_z = 0.2$. For the analysis we marginalize over the intrinsic magnitude $\mathcal{M}$.

4. Conclusion

We perform a Fisher matrix analysis to forecast the accuracy of the cosmological parameters as measured with the methods described in the previous sections. As a fiducial model we take the WMAP 1-year best fit model (Spergel et al. 2006) with $\Omega_m h^2 = 0.14$, $\Omega_{\rm DE} = 0.73$, $w_0 = -1$, $w_a = 0$, $\sigma_8 = 0.9$ (and $\sigma_8 = 0.75$ for the cluster counts), $\Omega_b h^2 = 0.024$, $n = 1$ and $\Omega_k = 0$. We want to emphasize that we do *not* restrict the analysis to flat models. We further employ prior information on the cosmological parameters from forecasts for the Planck Surveyor as provided by the DETF (Albrecht et al. 2006). In Fig. 2 we see the result of this analysis in the crucial w_0-w_a plane, marginalized over all other cosmological and nuisance parameters. This emphasizes the quality of the weak lensing and SNe measurements. The inverse figure of merit, can be expressed as $\sigma(w_p) \times \sigma(w_a)$, where w_p is the value of $w(z)$ at the best determined pivot redshift z_p. For the combined probes we find $\sigma(w_0) = 0.08$, $\sigma(w_a) = 0.28$ and a figure of merit of 200. This makes clear what a formidable probe of dark energy the DES would provide.

Acknowledgements. We would like to thank the DES collaboration for useful discussions. In particular we would like to mention F. Abdalla, S. Dodelson, W. Hu, D. Huterer and J. Tang. In addition we acknowledge useful discussions with R. Battye. We thank PPARC and institutional partners for their support of the DES project.

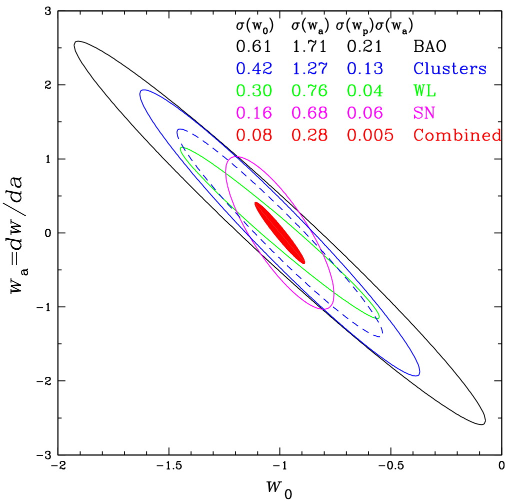

Fig. 2. 68% joint likelihood contours for the different DES probes and combined. This Figure was produced in collaboration with D. Huterer and J. Tang. From the outside in the solid lines are from BAO, cluster counts with $\sigma_8 = 0.75$, cluster counts with $\sigma_8 = 0.9$ (dashed), weak lensing and Supernovae. The filled contour is obtained when we combine the probes. The inset table in the Figure shows the accuracy of the measurement on w_0 and w_a and the inverse figure of merit $\sigma(w_p) \times \sigma(w_a)$, with w_p the best determined $w(z)$ at redshift z_p.

References

Albrecht, A., Bernstein, G., Cahn, R., et al., 2006, (astro-ph/0609591)
Battye, R. A. & Weller, J., 2003, Phys. Rev. D, 68, 083506
Cooray, A., Hu, W., Huterer, D., & Joffre, M., 2001, ApJ, 557, L7
Dodelson, S., Weller, J., & Battye, R. A., 2007, to be published
Hu, W., 2003, Phys. Rev. D, 67, 081304
Huterer, D., Takada, M., Bernstein, G., & Jain, B., 2006, MNRAS, 366, 101
Huterer, D. & White, M., 2002, ApJ, 578, L95
Jarvis, M. & Jain, B., 2004, (astro-ph/0412234)
Jenkins, A. et al., 2001, MNRAS, 321, 372
Kaiser, N., 1992, Astrophys. J., 388, 272
Lima, M. & Hu, W., 2004, Phys. Rev. D, 70, 043504
Linder, E. V., 2003, Physical Review Letters, 90, 091301
Ma, Z., Hu, W., & Huterer, D., 2006, ApJ, 636, 21
Majumdar, S. & Mohr, J. J., 2004, ApJ, 613, 41
Motl, P. M., Hallman, E. J., Burns, J. O., & Norman, M. L., 2005, ApJ, 623, L63
Nagai, D., 2006, ApJ, 650, 538
Ruhl, J., et al., 2004, in Astronomical Structures and Mechanisms Technology. Edited by Antebi, Joseph; Lemke, Dietrich. Proceedings of the SPIE, Volume 5498, pp. 11-29 (2004)., ed. J. Zmuidzinas, W. S. Holland, & S. Withington, 11–29
Sealfon, C., Verde, L., & Jimenez, R., 2006, ApJ, 649, 118
Sheth, R. K. & Tormen, G., 2002, MNRAS, 329, 61
Spergel, D. N., et al., 2006, ApJS, 170, 377
The Dark Energy Survey Collaboration., 2005, (astro-ph/0510346)
Verde, L., Haiman, Z., & Spergel, D. N., 2002, ApJ, 581, 5